Nitric Oxide Synthase Regulates Growth Coordination During *Drosophila melanogaster* Imaginal Disc Regeneration

Jacob S. Jaszczak, Jacob B. Wolpe, Anh Q. Dao, and Adrian Halme[1]

Department of Cell Biology, University of Virginia School of Medicine, Charlottesville, Virginia 22908

ABSTRACT Mechanisms that coordinate growth during development are essential for producing animals with proper organ proportion. Here we describe a pathway through which tissues communicate to coordinate growth. During *Drosophila melanogaster* larval development, damage to imaginal discs activates a regeneration checkpoint through expression of Dilp8. This both produces a delay in developmental timing and slows the growth of undamaged tissues, coordinating regeneration of the damaged tissue with developmental progression and overall growth. Here we demonstrate that Dilp8-dependent growth coordination between regenerating and undamaged tissues, but not developmental delay, requires the activity of nitric oxide synthase (NOS) in the prothoracic gland. NOS limits the growth of undamaged tissues by reducing ecdysone biosynthesis, a requirement for imaginal disc growth during both the regenerative checkpoint and normal development. Therefore, NOS activity in the prothoracic gland coordinates tissue growth through regulation of endocrine signals.

KEYWORDS regeneration; nitric oxide; ecdysone; allometry; growth control

ALLOMETRY, broadly defined as the scaling of organ growth, can have a profound impact on the biological function in animals. For example, in the male dung beetle, *Onthophagus netriventris*, an inverse allometry is observed between horn and testes size, producing distinct reproductive strategies (Simmons and Emlen 2006; Emlen *et al.* 2012). Allometric growth regulation can also impact human health where variation from optimal relative heart size can increase susceptibility to cardiovascular disease (Hill and Olson 2008). Despite the fundamental role of growth scaling in biology, no described pathways explain how tissues coordinate growth. Our understanding of growth regulation has been focused on either tissue-autonomous mechanisms—such as how morphogens regulate the activity of cellular growth pathways—or systemic mechanisms such as how endocrine factors control growth in response to environmental change.

These tissue-autonomous and systemic pathways of growth regulation do not explain allometric growth observed during development. Transplantation experiments (Madhavan and Schneiderman 1969) and growth perturbation experiments in *Drosophila* and other insects (Nijhout and Emlen 1998; Simmons and Emlen 2006; Parker and Shingleton 2011) suggest that interorgan communication may be necessary for allometric growth. Based on these observations, Stern and Emlen (1999) proposed a model for growth coordination that requires communication between growing organs, either directly or indirectly through an endocrine organ. However, the mechanism of this communication pathway has been unclear.

In *Drosophila* larvae, the growth of the imaginal discs is tightly regulated to produce adult structures with specific size and proportion (Mirth and Shingleton 2012; Callier and Nijhout 2013). Allometry between these tissues is preserved even when developmental growth programs are altered. For example, *Drosophila* imaginal discs have a remarkable capacity to regenerate and restore proper size and allometry following damage (Bryant 1971; Schubiger 1971). Damage to an imaginal disc activates a regeneration checkpoint (Halme *et al.* 2010) that extends the larval period of development (Rahn 1972; Dewes 1975; Simpson

et al. 1980; Poodry and Woods 1990; Halme et al. 2010), allowing time for regenerative tissue repair. Regeneration checkpoint activation also slows the growth rate of undamaged tissues (Madhavan and Schneiderman 1969; Stern and Emlen 1999; Martín and Morata 2006; Parker and Shingleton 2011), coordinating regeneration with the growth of undamaged imaginal discs. Both developmental delay and growth coordination depend on the expression of *Drosophila* insulin-like peptide 8 (Dilp8) in damaged tissues (Colombani et al. 2012; Garelli et al. 2012). Dilp8 is a secreted protein that shares structural features with the insulin/relaxin protein family. Several questions remain about how Dilp8 produces both growth regulation and developmental delay. It is possible that these two responses might be mechanistically linked; for example, growth restriction may lead to developmental delay (Poodry and Woods 1990; Stieper et al. 2008). Alternatively, these two systemic responses may reflect distinct Dilp8-dependent mechanisms. Additionally, it remains unclear whether Dilp8 functions to directly coordinate growth between tissues or whether Dilp8 mediates growth coordination indirectly through other systemic growth signals.

Nitric oxide synthase (NOS) produces nitric oxide (NO), a potent free radical that regulates many biological processes, including neuronal activity, immunity, and vascular regulation. Altering the activity of the sole NOS protein found in *Drosophila* produces changes in imaginal disc growth (Kuzin et al. 1996) and larval tissue growth (Cáceres et al. 2011). However, the mechanism of this regulation has remained unclear. In the experiments presented here, we outline a pathway through which tissues communicate with each other to produce allometric growth. We demonstrate that NOS activity is required for the Dilp8-dependent coordination of growth between regenerating and undamaged tissues following tissue damage and that NOS regulates growth in undamaged tissues by reducing ecdysone biosynthesis in the prothoracic gland.

Materials and Methods

Drosophila stocks

w*; P{UAS-Nos.L}2; P{UAS-Nos.L}3 was provided by Pat O'Farrell (Yakubovich et al. 2010); y,w; phm-GAL4{51A2} by Alexander Shingleton (Mirth et al. 2005); UAS-NOS^{mac} and UAS-NOS^{IR-X} by Henry Krause (Cáceres et al. 2011); NOS^1 by James Skeath (Lacin et al. 2014); UAS-eiger and UAS-reaper and rn-Gal4, UAS-YFP by Iswar Hariharan (Smith-Bolton et al. 2009); UAS-dilp8::3xFLAG by Maria Dominguez (Garelli et al. 2012); and UAS-Avl ^{RNAi} by David Bilder (Lu and Bilder 2005). All other stocks were obtained from the Bloomington *Drosophila* Stock Center or the Vienna *Drosophila* RNAi Center. Identifying stock numbers are referenced in the text.

Drosophila culture and media

Unless otherwise specified, larvae were reared at 25° on standard cornmeal–yeast–molasses media (Bloomington *Drosophila* Stock Center) supplemented with live baker's yeast granules. Developmental timing was synchronized through the collection of a 4-hr egg-laying interval on grape agar plates. Twenty hatched first instar larvae were transferred to vials containing media 24 hr after egg deposition (AED) (48 hr AED when raised at 21°). Heat shock-mediated expression was induced by 29° pretreatment and heat shock for 30 min at 37°. Nutrient restriction was initiated at 92 hr AED by transferring larvae to media containing only 1% agarose (Apex) in 1× PBS (pH 7.4, Sigma P4417) for the remainder of larval development.

Ionizing irradiation damage

Irradiation was performed as previously described (Halme et al. 2010). Briefly, staged larvae were raised in petri dishes on standard media and exposed to 25 Gy X-irradiation generated from a Faxitron RX-650 operating at 130 kV and 5.0 mA. For targeted irradiation experiments, shielded and control larvae were immobilized by being chilled in an ice bath, mounted on chilled glass coverslips, and kept on ice during the duration of the irradiation. Larvae were partially shielded from ionizing irradiation by placing a 0.5-cm^2 strip of lead tape (Gamma) over the estimated anterior third of their body, covering segments T1–T3. Larvae and control larvae were returned to cornmeal–molasses food at 25° following irradiation.

DAF2-DA assay

NO production was detected by 4,5-diaminofluorescein diacetate (DAF2-DA, Sigma). Brain complexes were dissected in PBS and incubated in 10 μM DAF2-DA for 1 hr at 28°, rinsed in PBS, stained with DAPI 1:1000, rinsed in PBS, and imaged by confocal microscopy. DAF2-DA fluorescence was quantified in ImageJ by measuring the mean gray value of each prothoracic gland (PG) lobe normalized to the background fluorescence of the adjacent brain hemisphere.

Additional methods and reagents are described in Supporting Information, File S1.

Results

NOS is necessary for growth regulation during the regeneration checkpoint

During larval development, imaginal disc damage activates a regeneration checkpoint that coordinates the regeneration of damaged imaginal tissues with developmental progression. Activation of the regeneration checkpoint produces both (1) delayed larval–pupal transition (Rahn 1972; Dewes 1975; Simpson et al. 1980; Poodry and Woods 1990; Halme et al. 2010) and (2) a reduced growth rate of undamaged imaginal tissues (Stern and Emlen 1999; Martín and Morata 2006; Parker and Shingleton 2011). Developmental delay and growth regulation have been shown to be dependent on Dilp8, but it has not been determined how Dilp8 reduces growth of undamaged imaginal tissues (Colombani et al. 2012; Garelli et al. 2012). We observe that growth coordination

between damaged and undamaged imaginal discs occurs when damage is induced by genetically targeted ablation of wing imaginal discs ($Bx > eiger$) or by exposing the posterior of the larva to X-irradiation (Figure 1, A–C, and Figure S1B for a description of the targeted irradiation technique). Consistent with earlier work (Colombani *et al.* 2012; Garelli *et al.* 2012), we find that both of these targeted damage models depend on the expression of *dilp8* from damaged tissues for growth coordination and developmental delay (Figure 1, B and C; Figure S1, C and D).

NOS regulates imaginal disc growth during *Drosophila* development (Kuzin *et al.* 1996), but the mechanism of this regulation is unknown. Therefore, we asked whether NOS is involved in Dilp8-dependent growth coordination. Using targeted irradiation, we observed that the reduced growth of shielded eye discs is rescued when larvae are homozygous for an amorphic allele of NOS [NOS^1 (Lacin *et al.* 2014)] (Figure 1D). Overexpression of Dilp8 is sufficient to reduce imaginal disc growth and produce developmental delay (Figure S1E) (Colombani *et al.* 2012; Garelli *et al.* 2012). To determine whether Dilp8-induced growth restriction is dependent on NOS, we measured growth of eye imaginal discs in *NOS* mutant larvae overexpressing Dilp8 in the wing imaginal discs ($Bx > dilp8;NOS^{1-/-}$). We observe that Dilp8-induced growth restriction is rescued in $NOS^{1-/-}$ mutant larvae (Figure 1E). Therefore NOS is required for growth coordination during the regeneration checkpoint, and Dilp8 is dependent on *NOS* for imaginal disc growth restriction.

Nitric oxide synthase activity in the prothoracic gland regulates imaginal disc growth

Consistent with previous observations (Kuzin *et al.* 1996), we find that a transient pulse of NOS expression ($hs > NOS$) early in the third larval instar (76 hr after egg deposition, AED) reduces imaginal disc growth. (Figure 2A and Figure S2A). However, overexpression of NOS within imaginal discs produces no observable effect on imaginal disc growth (Figure S2B), suggesting that NOS regulates growth via a nonautonomous pathway. Additionally, we observed that NOS induction following heat shock produces a developmental delay (Figure 2A and Figure S2A) without producing damage or apoptosis within the imaginal discs (Figure S2C).

The timing of developmental transitions in *Drosophila* larvae is regulated by the PG through pulsed production of the steroid hormone ecdysone (Warren *et al.* 2006). NOS expression in the PG has been demonstrated to regulate the larval-to-pupal transition by promoting ecdysone production in postfeeding larvae (Cáceres *et al.* 2011). However, when Cáceres *et al.* constitutively overexpressed NOS in the PG at 25° throughout larval development, they observed a delayed developmental progression and decreased larval size. Therefore, we examined whether NOS regulates growth through activity in the PG during the larval growth prior to the postfeeding phase of larval development. Using the *phantom-Gal4* driver, which specifically targets Gal4-mediated expression to
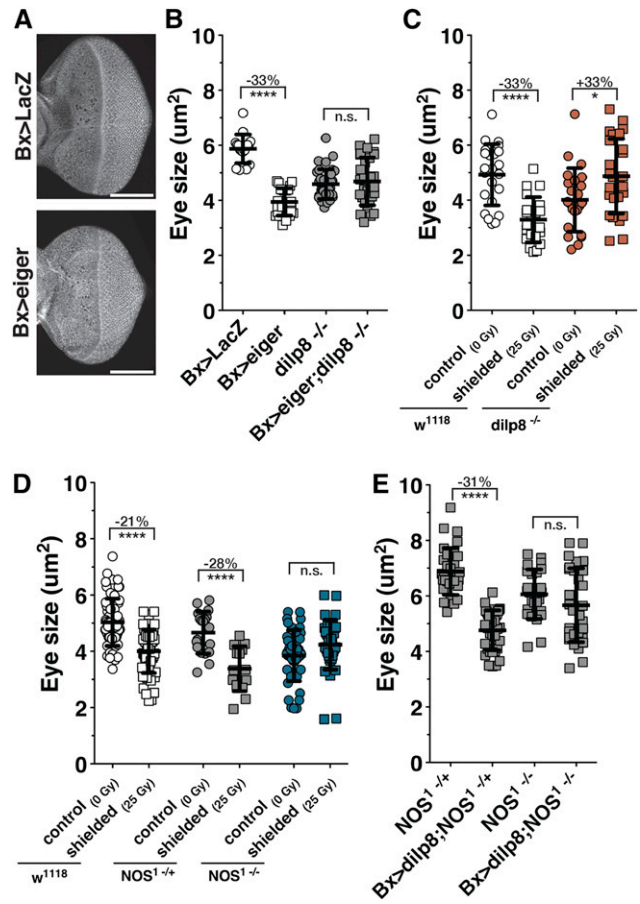
Figure 1 *NOS* is required for imaginal disc growth coordination during the regeneration checkpoint. (A) Growth reduction of undamaged eye imaginal discs in larvae with targeted tissue damage in the wings ($Bx > eiger$) and control larvae ($Bx > GFP$). Eyes were isolated at 104 hr AED and stained with rhodamine-labeled phalloidin. Bar, 100 μm. (B) *Dilp8* is required for coordinating imaginal tissue growth during targeted wing damage. Eye imaginal disc size measured at 104 hr AED following targeted wing expression of eiger ($Bx > eiger$) or control ($Bx > LacZ$) in larvae wild type for *dilp8* or homozygous *dilp8*$^{-/-}$. (C) *Dilp8* is required for coordinating imaginal tissue growth during irradiation damage. Measurement of undamaged eye imaginal disc size following targeted irradiation (shielded, 25 Gy) compared to unirradiated control (0 Gy) in wild type (w^{1118}) and homozygous *dilp8*$^{-/-}$ larvae. Posterior tissues were exposed to 25 Gy ionizing irradiation at 80 hr AED while anterior tissues were shielded using lead tape (see *Materials and Methods* and Figure S1B for more detail). Eye imaginal disc size measured at 104 hr AED. (D) *NOS* is required for coordinating imaginal tissue growth during the regeneration checkpoint. Coordination of growth during targeted irradiation is lost in larvae mutant for *NOS*. Measurement of undamaged eye imaginal disc size following targeted irradiation compared to unirradiated control in wild type (w^{1118}) and larva heterozygous or homozygous for *NOS* mutant (NOS^1). Posterior tissues were exposed to irradiation at 80 hr AED, and eye imaginal disc size was measured at 104 hr AED. (E) Dilp8 growth restriction requires *NOS*. Eye imaginal disc growth restriction during *dilp8* overexpression in the wing ($Bx > dilp8$) is lost in larvae mutant for *NOS* (NOS^1 $^{-/-}$). Larvae were raised at 29°, and eye imaginal disc size was measured at 100 hr AED. Statistical analysis: mean ± SD. *$P < 0.05$, ****$P < 0.001$ calculated by two-tailed Student's *t*-test.

the PG throughout larval development (Mirth *et al.* 2005), we observed that most *phm* > *NOS* larvae raised at 25° died prior to the third larval instar. To determine if larval lethality
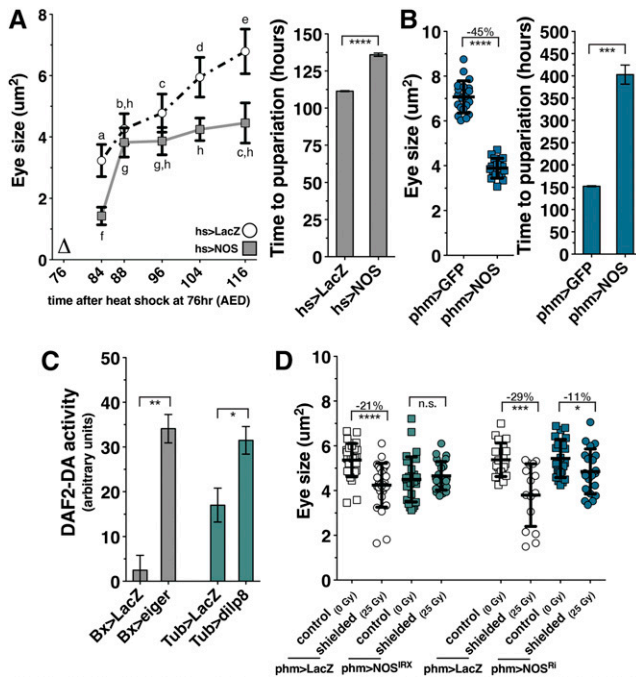
Figure 2 *NOS* is required in the PG to coordinate imaginal tissue growth during the regeneration checkpoint. (A) A systemic pulse of *NOS* expression early during the larval feeding period restricts imaginal disc growth throughout the rest of larval development. *NOS* was systemically expressed by heat shock (Δ) at 76 hr AED, and eye imaginal disc size was measured in populations of larva at subsequent time points. *NOS* overexpression at 76 hr AED extends larval development. Measurement of pupariation timing (marked by eversion of anterior spiracles) following systemic expression of *NOS* (*hs > NOS*) is depicted on the right. (B) *NOS* overexpression in the PG (*phm > NOS*) restricts imaginal disc growth and extends larval development. *phm > GFP-* and *phm > NOS*-expressing larvae were raised at 21° (see Figure S2D). (C) Both targeted tissue damage (*Bx > eiger*) and systemic *dilp8* expression (*Tub > dilp8*) increase NO production in the PG. Measurement of NO production by the fluorescent reporter DAF2-DA. Brain complexes with the PG attached were isolated and stained with DAPI and DAF2-DA at 93 hr AED. *n* for *Bx > LacZ* = 36, *Bx > eiger* = 23, *Tub > LacZ* = 20, and *Tub > dilp8* = 23. (D) *NOS* is required in the PG for regeneration checkpoint growth coordination. Measurement of undamaged eye imaginal disc size following shielded irradiation (25 Gy) compared to unirradiated control (0 Gy) in control (*phm > LacZ*) or NOS-targeted RNAi expressed in the PG (*phm > NOS^{IR-X}* or *phm > NOS^{Ri BL28792}*). Posterior tissues were exposed to 25 Gy ionizing irradiation at 80 hr AED and anterior tissues, including the eye discs, were shielded using lead tape. Eye imaginal disc size was measured at 104 hr AED. Statistical analysis: (A) Differing letters denote statistical significance calculated by one-way ANOVA with Tukey's post-test. (B) Mean ± SD. Time in A and B is the mean of triplicate experiments ± SEM. (C) Mean of triplicate experiments. (D) Mean ± SD. *$P < 0.05$, **$P < 0.01$, ***$P < 0.005$, and ****$P < 0.001$ calculated by two-tailed Student's *t*-test.

could be rescued by reducing the expression of NOS in the PG, we raised *phm > NOS* and control larvae at 21°, which reduces GAL4 activity and slows developmental time (Figure S2D). The majority of *phm > NOS* larvae raised at 21° progressed through the third instar to pupation (Figure S2E). We observed that in these *phm > NOS* larvae the growth rate of the eye imaginal tissues is reduced relative to control

larvae raised at 21° (Figure 2B). The pupation of these larvae is also delayed in comparison to control larvae (Figure 2C). Therefore, *NOS* overexpression in the PG is sufficient to reduce the growth of imaginal discs during the third larval instar and can delay the exit from larval development.

NOS catalyzes the production of the free radical nitric oxide (NO), an important cellular signaling molecule, from L-arginine. To determine whether NOS activity is increased in the PG during the regeneration checkpoint, we used the fluorescent reporter molecule DAF2-DA to measure NO production, as can be observed in the PG of *phm > NOS* larvae (Figure S3). Larva with genetically targeted wing ablation (*Bx > eiger*) or systemic Dilp8 misexpression produce increased levels of NO signaling in the PG compared to control larvae (Figure 2C), demonstrating that the regeneration checkpoint acts through Dilp8 to increase NOS activity in the PG. To examine whether this activation of NOS in the PG is required for the regeneration checkpoint growth coordination, we expressed a NOS-targeted RNAi to disrupt NOS function in the PG using the *phm-GAL4* driver [*phm > NOS^{IR-X}* (Cáceres *et al.* 2011) or *phm > NOS^{Ri}* (Bloomington #28792)]. Using the targeted irradiation technique, we observed that depletion of *NOS* in the PG by RNAi restored eye imaginal disc growth in shielded larvae to the rate observed in unirradiated larvae (Figure 2D). Therefore, nitric oxide production is increased in the PG during the regeneration checkpoint, and *NOS* activation in the PG is necessary to regulate imaginal tissue growth during the regeneration checkpoint.

Growth regulation during the regeneration checkpoint is dependent on NOS. However, we observed no effect on the delay of development induced by irradiation in *NOS* RNAi knockdown or in the *NOS* mutant larvae (Figure 3, A and B). These data suggest that overexpression of *NOS* (Figure 2, A and B) delays development through a mechanism distinct from the regeneration checkpoint. Together, these data demonstrate that localized imaginal disc damage produces two effects: (1) growth inhibition in undamaged imaginal tissues, which is dependent on NOS function in the PG, and (2) a delay in developmental timing, which occurs through a NOS-independent pathway.

Growth of imaginal tissues is selectively regulated during the regeneration checkpoint

Larval size is determined by the growth of polyploid larval tissues such as the larval epidermis, fat body, and salivary glands (Oldham *et al.* 2000). Unlike the diploid imaginal tissues, which will become much of the adult fly following metamorphosis, most larval tissues are histolysed during metamorphosis and do not contribute significantly to the adult. To determine whether imaginal tissues are selectively targeted for growth regulation during the regeneration checkpoint, we compared the effects of regeneration checkpoint activation on the growth of both imaginal tissues and total larval size, which correlates with the growth of the
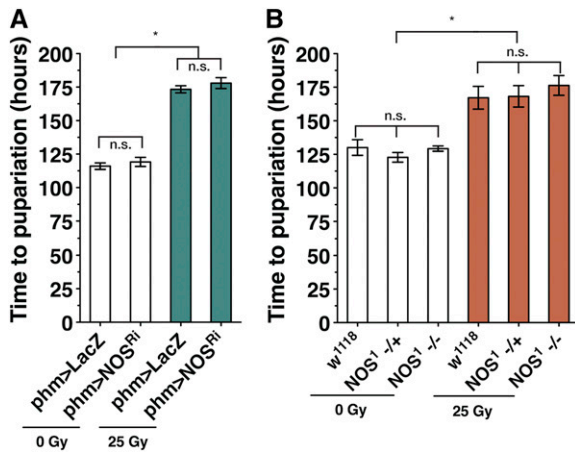
Figure 3 *NOS* is not required for regulation of developmental time during the regeneration checkpoint. Loss of *NOS* function either by (A) knockdown of *NOS* in the PG (*phm > NOS*[Ri]) or (B) *NOS* mutant (*NOS*[1]) does not alter developmental delay. Measurement of pupariation timing for larvae with irradiation damage (25 Gy) and control larvae (0 Gy). Mean of triplicates ± SEM. *P < 0.05 calculated by one-way ANOVA with Tukey's post-test.

polyploid larval epidermis (Cheng *et al.* 2011). Consistent with our earlier observations, targeted irradiation or genetically targeted ablation of wing imaginal discs (*Bx > eiger*) is sufficient to activate the regeneration checkpoint and produce growth inhibition of undamaged eye imaginal discs (Figure S4, A and B). Both damage models depend on Dilp8 for growth inhibition and developmental delay (Figure 1 and Figure S1). Consistent with a role for NOS and Dilp8 in growth regulation during the regeneration checkpoint, we observe growth inhibition of undamaged eye imaginal tissues by expression of *NOS* in the PG (*phm > NOS*, Figure S4B) and *dilp8* expression in the wing pouch, the region of the imaginal disc that will become the adult wing blade (*rn > dilp8*, Figure S4B).

In stark contrast, we found that checkpoint activation does not reduce overall larval growth (Figure S4, C and D). In our two damage models, larval growth continued at the same rate or even slightly faster than the growth observed in control larvae. Similarly, we observed a slight but not statistically significant increase in the rate of larval tissue growth in larvae with *phm > NOS* and wing-targeted expression of Dilp8 (*rn > dilp8*), as compared with control larvae (Figure S4D). Additionally, we examined other disruptions of wing imaginal disc growth and found that induction of neoplastic tumors in the wing imaginal tissues using knockdown of the *Drosophila* syntaxin protein Avalanche [*Bx > avl*[RNAi] (Lu and Bilder 2005)] also produces slower growth in the eye imaginal discs without altering larval tissue growth (Figure S4, B and D). This is consistent with the observed activation of Dilp8 during tumorigenesis (Colombani *et al.* 2012; Garelli *et al.* 2012). This pattern of growth regulation observed during the regeneration checkpoint—*i.e.*, reduced growth of imaginal discs and sustained or even increased growth of larval tissues —contrasts with the growth pattern observed

in larvae with reduced insulin signaling in response to nutrient restriction, where growth of both imaginal and larval tissues is reduced (Figure S4, B and D). Therefore, we sought to test a growth regulatory pathway other than insulin signaling that would explain how regenerative checkpoint activation and NOS activity could specifically reduce imaginal disc growth.

NOS in the PG inhibits ecdysone biosynthesis during the larval growth phase

The PG produces pulses of ecdysone synthesis during the larval growth phase that determine the timing of developmental transitions such as larval molts, the mid-third instar transition (Andres and Cherbas 1992), critical weight (Koyama *et al.* 2014), and the exit from larval development. Experiments support roles for ecdysone in both promoting (Nijhout *et al.* 2007; Delanoue *et al.* 2010; Nijhout and Grunert 2010; Parker and Shingleton 2011) and restricting (Colombani *et al.* 2005; Mirth *et al.* 2005; Delanoue *et al.* 2010; Nijhout and Grunert 2010; Boulan *et al.* 2013) growth of imaginal discs. Activation of the regeneration checkpoint slows the progression of the morphogenetic furrow in undamaged eye discs (see Figure S4A). Furrow progression is dependent on ecdysone (Brennan *et al.* 1998), and therefore its slowed progression is consistent with the regeneration checkpoint reducing ecdysone signaling during larval development. Since the overexpression of NOS in the PG influences both developmental timing and imaginal disc growth, we examined whether NOS activity in the PG alters ecdysone signaling during the regeneration checkpoint.

Regeneration checkpoint activation has been shown to reduce ecdysone biosynthesis (Hackney *et al.* 2012). To examine whether NOS activity in the PG reduces ecdysone production, we measured ecdysteroid levels using a competitive enzyme immunoassay (Porcheron *et al.* 1989). In larvae overexpressing NOS in the PG (*phm > NOS*), we observed a strong reduction in ecdysteroid levels during the mid-third instar when imaginal disc growth is rate reduced (Figure 4A). To determine whether ecdysone signaling is reduced during this period, we measured transcription of the ecdysone target gene *E74B* (Colombani *et al.* 2005; Parker and Shingleton 2011; Hackney *et al.* 2012). In *phm > NOS*-expressing larvae we observed that the expression of E74B is lower than in control larvae during the mid- and late third instar (Figure 4B), suggesting that ecdysone titers are reduced during this period. Consistent with previous studies (Hackney *et al.* 2012), we observed that transcription of *E74B* is reduced following activation of the regeneration checkpoint in *Bx > eiger* larvae (Figure S5A). Together, these results demonstrate that ecdysone production is reduced when NOS is active in the PG during the third instar larval growth period.

To better understand how NOS reduces ecdysone production in larvae, we examined whether NOS regulates the expression of ecdysone biosynthetic genes. Ecdysone is synthesized in the PG from sterol precursors
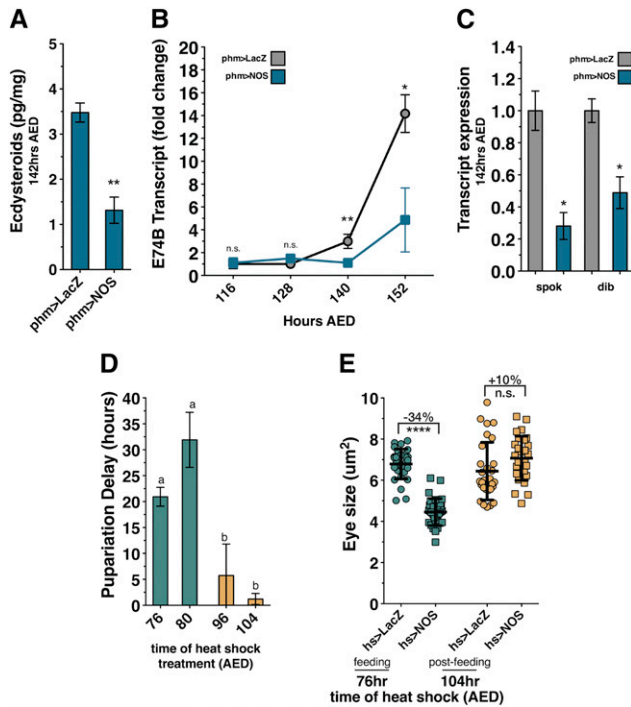
Figure 4 *NOS* overexpression during larval feeding inhibits ecdysone biosynthesis. (A) NOS activity in the PG reduces ecdysteroid production. The presence of ecdysteroids is reduced in larvae with *NOS* overexpression in the PG (*phm* > *NOS*) compared to control (*phm* > *LacZ*) larvae. Ecdysone levels were measured by ELISA assay for independent isolation triplicates. (B) *NOS* expression in the PG reduces ecdysone signaling. Transcription of *E74B* is reduced in larvae with *NOS* overexpression in the PG (*phm* > *NOS*) compared to control (*phm* > *LacZ*) larvae. Transcription levels measured by qRT-PCR in triplicate, normalized to control expression levels at 116 hr AED. (C) *NOS* activity in the PG reduces Halloween gene transcription. Relative expression of *spok* and *dib* in control (*phm* > *LacZ*) larvae and larvae with *NOS* overexpression in the PG (*phm* > *NOS*) are depicted. Transcription levels were measured by qRT-PCR in triplicate, normalized to control transcription levels. (D) Expression of *NOS* early during the larval feeding period (76 and 80 hr AED) substantially delays larval development, while *NOS* expression late during the wandering period (96 and 104 hr AED) does not delay development. *NOS* was systemically expressed by heat shock (*hs* > *NOS*) once at 76, 80, 96, or 104 hr AED, and time to pupariation was measured. (E) Expression of *NOS* early during the larval feeding period restricts imaginal disc growth, while *NOS* expression late during the wandering period does not inhibit growth. *NOS* was systemically expressed by heat shock (*hs* > *NOS*) at either 76 or 104 hr AED, and eye imaginal disc size was measured at 116 hr AED. All *phm* > *LacZ*- and *phm* > *NOS*-expressing larvae were raised at 21°. Statistical analysis: A and E, mean of triplicates ± SD calculated by two-tailed Student's *t*-test. (B and C) Mean of triplicates ± SEM, calculated by paired one-tailed *t*-test. (D) Mean of triplicates ± SEM. *$P < 0.05$, **$P < 0.01$, ****$P < 0.001$.

by the consecutive actions of the P450 enzymes collectively referred to as "the Halloween enzymes" (Gilbert and Rewitz 2009). Previous work has demonstrated that the expression of Halloween genes is reduced during activation of the regeneration checkpoint (Hackney *et al.* 2012). To determine whether NOS regulates ecdysone synthesis by limiting Halloween gene expression, we examined the transcription of the Halloween genes *spookier*

(*spok*) (Ono *et al.* 2006) and *disembodied* (*dib*) during either targeted tissue damage or NOS overexpression in the PG (Chávez *et al.* 2000). Transcription of both *spok* and *dib* is reduced in *phm* > *NOS* larvae in comparison to control larvae (Figure 4C), consistent with the reductions observed during regeneration checkpoint activation (Figure S5A). Therefore, upon activation of the regeneration checkpoint, NOS functions in the PG to reduce ecdysone signaling through the transcriptional repression of ecdysone biosynthesis genes.

This model contrasts with a model arising from previous work demonstrating that NOS activity in the PG of postfeeding larvae inhibits the nuclear hormone receptor *E75*, an antagonist of ecdysone biosynthesis (Cáceres *et al.* 2011). To reconcile these two distinct descriptions of NOS activity in the PG, we first sought to determine whether this E75-dependent pathway of ecdysone regulation is active during the earlier growth phase of larval development. We observed that the *E75B* expression, which is normally upregulated during the postfeeding period of larval development, is completely suppressed in larvae with targeted wing damage (Figure S5B). Therefore, we conclude the E75-dependent pathway is not likely to be active during the growth phase of larval development and is delayed following activation of the regeneration checkpoint. Consistent with this, the ability of transient *NOS* misexpression (*hs* > *NOS*) to delay pupation is most robust when expressed during larval feeding (76 or 80 hr). This delay is significantly decreased when *NOS* was misexpressed later in the third instar as the larvae entered the postfeeding phase (96 or 104 hr) (Figure 4D). These results suggest that the ecdysone-inhibiting and ecdysone-promoting mechanisms of NOS are temporally separated during the larval growth and postfeeding phases of development.

To further test whether NOS activity is dependent on developmental stage of the larvae, we examined whether the reduction of imaginal disc growth induced by transient misexpression of *NOS* (*hs* > *NOS*) is dependent on the stage of development. We observed that misexpressing *NOS* early in the third instar during the larval feeding period (76 hr AED) produces a robust restriction of imaginal disc growth (Figure 4E, 76 hr). However, we found that misexpression of *NOS* late in the third instar, at the time that larvae stop feeding (104 hr AED), produces minimal effect on developmental time and imaginal disc growth (Figure 4, D and E, 104 hr). In fact, a slight increase in growth was measurable. Consistent with this, we also observed decreases in *E74B* and *dib* transcription after early *NOS* misexpression in contrast to an increase in *spok* transcription resulting from late *NOS* misexpression (Figure S5, C and D). These results suggest that as development progresses the regulatory effect of NOS in the PG has two distinct states. During the feeding phase of larval development, NOS inhibits ecdysone production as we describe here. Later in postfeeding larvae, as described in Cáceres *et al.* (2011), NOS functions to promote ecdysone signaling by inhibiting E75 activity.

Regeneration checkpoint reduces growth of undamaged tissues by limiting ecdysone signaling

We then determined whether the reduced growth of undamaged discs during regeneration checkpoint activation is the result of reduced ecdysone production. Feeding larvae food supplemented with ecdysone (0.6 mg/ml) increases ecdysone titer in larvae (Colombani *et al.* 2005). Using this approach, we tested whether we could bypass NOS-dependent growth inhibition by ecdysone feeding. We observed that ecdysone feeding can bypass the imaginal disc growth restriction produced by (1) imaginal tissue damage (*Bx* > *eiger*, Figure 5A), (2) regeneration checkpoint signaling (*Tub* > *dilp8*, Figure 5B), or (3) transient misexpression of *NOS* (*hs* > *NOS*, Figure 5C and Figure S6A) and *NOS* activity in the PG (*phm* > *NOS*, Figure 5D). Ecdysone feeding did not significantly alter the growth of larval tissues during damage or NOS overexpression, but strongly reduced larval tissue growth in *dilp8*-misexpressing larvae, as reflected in the overall larval size (Figure S6C).

To determine whether ecdysone promotes imaginal disc growth during normal development, we reduced ecdysone levels in third instar larvae by transferring larvae to yeast–sucrose food prepared using $erg6^{-/-}$ mutant yeast, which lacks the necessary steroid precursors for ecdysone synthesis (Bos *et al.* 1976; Parkin and Burnet 1986) (see *Materials and Methods*). This resulted in a marked decrease in imaginal tissue growth (Figure S6D); an extended developmental time to pupation (Figure S6E); and a slight, but significant, increase in larval tissue growth (Figure S6F) as compared with control larvae. Therefore, ecdysone is required for a normal rate of imaginal disc growth during the third instar even in the absence of imaginal disc damage. Furthermore, we observed that ecdysone limitation by growth on $erg6^{-/-}$ food produces only a minor effect on the growth of imaginal tissues in *Bx* > *eiger* larvae (Figure S6D). This epistatic interaction supports a model in which the regeneration checkpoint and ecdysone regulate imaginal tissue growth via convergent mechanisms. Together, these results demonstrate that the regeneration checkpoint limits undamaged imaginal disc growth through NOS-dependent reduction of ecdysone synthesis.

Discussion

During *Drosophila* development, damage to larval imaginal discs elicits a regeneration checkpoint that has two effects: (1) it delays the exit from the larval phase in development to extend the regenerative period and (2) it coordinates regenerative growth with the growth of undamaged tissues by slowing the growth rate of distal, undamaged tissues. How regenerating tissues communicate with undamaged tissues to coordinate growth has been an open question. Damaged tissues may produce signals that directly influence the growth of undamaged tissues or may indirectly influence the growth of undamaged tissues by producing signals that alter the levels of limiting growth factors. Consistent with
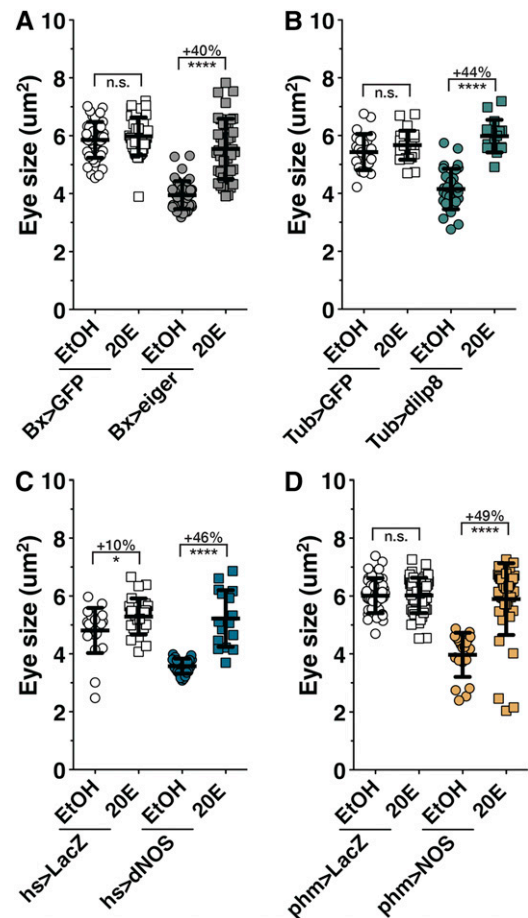
Figure 5 Imaginal disc growth restriction during the regeneration checkpoint is the result of reduced ecdysone signaling. Ecdysone levels are rate-limiting for imaginal disc growth during the regeneration checkpoint. 20-Hydroxyecdysone (20E) rescues growth restriction induced by (A) targeted wing damage (*Bx* > *eiger*), (B) systemic *dilp8* misexpression (*Tub* > *dilp8*), (C) systemic *NOS* misexpression (*hs* > *NOS*), and (D) PG *NOS* overexpression (*phm* > *NOS*) compared to control ethanol fed only larvae (EtOH). Statistical analysis: mean ± SD. *$P < 0.05$ and ****$P < 0.001$ calculated by two-tailed Student's t-test.

the latter model, we describe an indirect-communication pathway for growth coordination during the regeneration checkpoint (Figure 6).

An essential component of this growth coordination is the secreted peptide Dilp8, which is released by damaged tissues and is both necessary and sufficient to regulate the growth of distal tissues during the regeneration checkpoint (Colombani *et al.* 2012; Garelli *et al.* 2012). Dilp8 shares structural similarity to insulin-like peptides, which function to stimulate growth by activating the insulin receptor. However, in contrast to insulin-like peptides, Dilp8 acts to limit growth. A simple model explaining Dilp8 function would be that Dilp8 acts directly as an antagonist to insulin receptor activity, thus reducing growth in undamaged tissues. However, we show that the growth response to checkpoint activation of polyploid larval tissues differs from imaginal discs (Figure S4). The growth of polyploid larval tissues is very
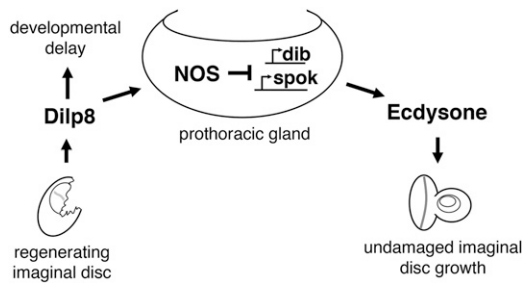
Figure 6 Model for allometric growth regulation during the regeneration checkpoint. Growth is coordinated between regenerating and undamaged imaginal discs through the PG. During the larval growth period, Dilp8 secreted from regenerating imaginal discs activates nitric oxide synthase in the prothoracic gland, inhibiting ecdysone biosynthesis and reducing undamaged imaginal disc growth. Dilp8-dependent developmental delay is produced through a NOS-independent mechanism.

sensitive to changes in insulin signaling; therefore, these results are inconsistent with Dilp8 regulating imaginal disc growth by antagonizing systemic insulin signaling.

We show here that NOS functions in the PG to regulate the growth of imaginal discs during the developmental checkpoint. We demonstrate that growth coordination during the regeneration checkpoint increases NO production in the PG and is dependent on *NOS* gene function in the PG. Although constitutive expression of NOS in the PG might produce effects earlier in development that might alter our interpretations, we also demonstrate that both transient pulses of NOS during the third instar and targeted NOS activation in the PG produce the same effects: inhibition of imaginal disc growth by limiting ecdysone signaling. We show that NOS activity in the PG reduces ecdysone production through the transcriptional inhibition of the P450 enzymes *disembodied* and *spookier*, which are necessary for ecdysone biosynthesis. Although it has been known that NOS activity is capable of regulating growth of imaginal discs (Kuzin *et al.* 1996), the experiments that we describe here elucidate the mechanism of this growth regulation.

The activity of NOS described here contrasts with published experiments demonstrating that NO signaling inhibits E75 activity in the PG, thus promoting larval exit (Cáceres *et al.* 2011). However, experiments from Caceres *et al.* demonstrate that earlier *NOS* expression in the PG during larval development produces small larvae that arrest at the second larval instar stage of development. This arrest can be partially rescued either by ecdysone feeding (Cáceres *et al.* 2011) or by reducing the level of GAL4-UAS-driven *NOS* expression by raising larvae at a lower temperature (Figure S2E). Additionally, pharmacological increase of NO levels in larvae can produce larval developmental delays (Lozinsky *et al.* 2012, 2013). Together, these observations suggest that NOS activity earlier in larval development might inhibit rather than promote ecdysone signaling during the larval growth period. Finally, we observe that *E75B* is not expressed in larvae that have activated the regenerative checkpoint (Figure S5B), suggesting that the NOS-dependent pathway that has been

described by Cáceres *et al.* (2011) is not active during the regeneration checkpoint.

We have focused on the role of NOS during the growth phase of the third larval instar (76–104 hr AED) and have found that heat-shock-mediated pulses of NOS activity during this period of development inhibit growth and ecdysone signaling, while pulses of NOS activity at the end of larval development do not inhibit growth or ecdysone signaling (Figure 4). Based on these results, we conclude that there are distinct roles for NOS in the PG during different phases in development; NOS activity during postlarval feeding promotes ecdysone synthesis through inhibition of *E75*, whereas NOS activity during the larval growth phase limits ecdysone synthesis and signaling by reducing the expression of ecdysone biosynthesis genes through a yet-to-be defined mechanism. Some possible mechanisms are through regulation of the growth of the PG or via activation of cGMP-dependent pathways.

Furthermore, we demonstrate that ecdysone is essential for imaginal disc growth. Most studies have supported a model in which ecdysone acts as a negative regulator of growth based on two observations: (1) the final pulse of ecdysone at the end of the third larval instar shortens developmental time and therefore reduces final organ size and (2) increased ecdysone signaling can antagonize Dilp synthesis in the fat body (Colombani *et al.* 2005; Mirth *et al.* 2005; Delanoue *et al.* 2010; Nijhout and Grunert 2010; Boulan *et al.* 2013). However, when measuring the effects of ecdysone on growth, many previous studies have focused on measuring either the growth of the larvae (which, as we observe, does not always reflect the growth of the imaginal tissues) or on measuring the final size of adults (a function of both growth rate and time). When one either examines clones expressing mutant alleles of ecdysone receptor (Delanoue *et al.* 2010) or measures the growth of entire imaginal discs directly following ecdysone feeding as we have done here, ecdysone signaling can be shown to promote imaginal disc growth.

During the regeneration checkpoint, both growth coordination and the delay in developmental timing are dependent on reduced ecdysone levels. Therefore, we might expect both delay and growth inhibition to be dependent on the same pathways. However, we clearly demonstrate that the genetic requirements for these two systemic responses to damage are distinct. NOS is necessary for growth regulation following tissue damage, but is not necessary for the developmental delay. While we do observe that overexpression of NOS in the PG produces developmental delay, our results suggest that this is through a mechanism different from the delays produced during the regeneration checkpoint. Therefore, Dilp8 secretion from damaged imaginal discs produces developmental delay and growth restriction through distinct mechanisms.

Finally, our observations suggest that regenerative growth, which is able to proceed despite reduced ecdysone signaling, may have different growth requirements than undamaged

tissues. Understanding these differences in growth regulation could provide valuable insights into the mechanistic distinctions between regenerative and developmental growth.

Acknowledgments

Literature Cited

Andres, A. J., and P. Cherbas, 1992   Tissue-specific ecdysone responses: regulation of the Drosophila genes Eip28/29 and Eip40 during larval development. Development 116: 865–876.

Bos, M., B. Burnet, R. Farrow, and R. A. Woods, 1976   Development of Drosophila on sterol mutants of the yeast Saccharomyces cerevisiae. Genet. Res. 28: 163–176.

Boulan, L., D. Martín, and M. Milán, 2013   Bantam miRNA promotes systemic growth by connecting insulin signaling and ecdysone production. Curr. Biol. 23: 473–478.

Brennan, C. A., M. Ashburner, and K. Moses, 1998   Ecdysone pathway is required for furrow progression in the developing Drosophila eye. Development 125: 2653–2664.

Bryant, P. J., 1971   Regeneration and duplication following operations in situ on the imaginal discs of Drosophila melanogaster. Dev. Biol. 26: 637–651.

Cáceres, L., A. S. Necakov, C. Schwartz, S. Kimber, I. J. H. Roberts et al., 2011   Nitric oxide coordinates metabolism, growth, and development via the nuclear receptor E75. Genes Dev. 25: 1476–1485.

Callier, V., and H. F. Nijhout, 2013   Body size determination in insects: a review and synthesis of size- and brain-dependent and independent mechanisms. Biol. Rev. Camb. Philos. Soc. 88: 944–954.

Chávez, V. M., G. Marqués, J. P. Delbecque, K. Kobayashi, M. Hollingsworth et al., 2000   The Drosophila disembodied gene controls late embryonic morphogenesis and codes for a cytochrome P450 enzyme that regulates embryonic ecdysone levels. Development 127: 4115–4126.

Cheng, L. Y., A. P. Bailey, S. J. Leevers, T. J. Ragan, P. C. Driscoll et al., 2011   Anaplastic lymphoma kinase spares organ growth during nutrient restriction in Drosophila. Cell 146: 435–447.

Colombani, J., L. Bianchini, S. Layalle, E. Pondeville, C. Dauphin-Villemant et al., 2005   Antagonistic actions of ecdysone and insulins determine final size in Drosophila. Science 310: 667–670.

Colombani, J., Andersen D. S., and Leopold P., 2012   Secreted peptide Dilp8 coordinates Drosophila tissue growth with developmental timing. Science 336: 582–585.

Delanoue, R., M. Slaidina, and P. Léopold, 2010   The steroid hormone ecdysone controls systemic growth by repressing dMyc function in Drosophila fat cells. Dev. Cell 18: 1012–1021.

Dewes, E., 1975 Entwicklungsleistungen Implantierter Ganzer und Halbierter Männlicher Genitalimaginalscheiben von Ephestia kuehniella Z. und Entwicklungsdauer der Wirtstiere. Wilhelm Roux' Arch. 178: 167–183.

Emlen, D. J., and I. A. Warren, A. Johns, I. Dworkin, and L. C. Lavine, 2012   A mechanism of extreme growth and reliable signaling in sexually selected ornaments and weapons. Science 337: 860–864.

Garelli, A., A. M. Gontijo, V. Miguela, E. Caparros, and M. Dominguez, 2012   Imaginal discs secrete insulin-like peptide 8 to mediate plasticity of growth and maturation. Science 336: 579–582.

Gilbert, L. I., and K. F. Rewitz, 2009   The function and evolution of the Halloween genes: the pathway to the arthropod molting hormone, pp. 231–269 in Ecdysone: Structures and Functions. Springer, New York.

Hackney, J. F., O. Zolali-Meybodi, and P. Cherbas, 2012   Tissue damage disrupts developmental progression and ecdysteroid biosynthesis in Drosophila. PLoS One 7: e49105.

Halme, A., M. Cheng, and I. K. Hariharan, 2010   Retinoids regulate a developmental checkpoint for tissue regeneration in Drosophila. Curr. Biol. 20: 458–463.

Hill,, J. A., and E. N. Olson, 2008   Cardiac plasticity. N. Engl. J. Med. 358: 1370–1380.

Koyama, T., and M. A. Rodrigues, A. Athanasiadis, A. W. Shingleton, and C. K. Mirth, 2014   Nutritional control of body size through FoxO-Ultraspiracle mediated ecdysone biosynthesis. eLife 3: 1–20.

Kuzin, B., I. Roberts, N. Peunova, and G. Enikolopov, 1996   Nitric oxide regulates cell proliferation during Drosophila development. Dev. Cell 87: 639–649.

Lacin, H., J. Rusch, R. T. Yeh, M. Fujioka, B. A. Wilson et al., 2014   Genome-wide identification of Drosophila Hb9 targets reveals a pivotal role in directing the transcriptome within eight neuronal lineages, including activation of nitric oxide synthase and Fd59a/Fox-D. Dev. Biol. 388: 117–133.

Lozinsky, O. V., O. V. Lushchak, J. M. Storey, K. B. Storey, and V. I. Lushchak, 2012   Sodium nitroprusside toxicity in Drosophila melanogaster: delayed pupation, reduced adult emergence, and induced oxidative/nitrosative stress in eclosed flies. Arch. Insect Biochem. Physiol. 80: 166–185.

Lozinsky, O. V., O. V. Lushchak, N. I. Kryshchuk, N. Y. Shchypanska, A. H. Riabkina et al., 2013   S-nitrosoglutathione-induced toxicity in Drosophila melanogaster: delayed pupation and induced mild oxidative/nitrosative stress in eclosed flies. Comp. Biochem. Physiol. A Mol. Integr. Physiol. 164: 162–170.

Lu, H., and D. Bilder, 2005   Endocytic control of epithelial polarity and proliferation in Drosophila. Nat. Cell Biol. 7: 1232–1239.

Madhavan, K., and H. Schneiderman, 1969   Hormonal control of imaginal disc regeneration in Galleria mellonella (Lipidoptera). Biol. Bull. 137: 321–331.

Martín, F. A., and G. Morata, 2006   Compartments and the control of growth in the Drosophila wing imaginal disc. Development 133: 4421–4426.

Mirth, C. K., and A. W. Shingleton, 2012   Integrating body and organ size in Drosophila: recent advances and outstanding problems. Front. Endocrinol. (Lausanne) 3: 1–13.

Mirth, C., J. W. Truman, and L. M. Riddiford, 2005   The role of the prothoracic gland in determining critical weight for metamorphosis in Drosophila melanogaster. Curr. Biol. 15: 1796–1807.

Nijhout, H. F., and D. J. Emlen, 1998   Competition among body parts in the development and evolution of insect morphology. Proc. Natl. Acad. Sci. USA 95: 3685–3689.

Nijhout, H. F., and L. W. Grunert, 2010   The cellular and physiological mechanism of wing-body scaling in Manduca sexta. Science 330: 1693–1695.

Nijhout, H. F., W. A. Smith, I. Schachar, S. Subramanian, A. Tobler et al., 2007   The control of growth and differentiation of the wing imaginal disks of Manduca sexta. Dev. Biol. 302: 569–576.

Oldham, S., J. Montagne, T. Radimerski, G. Thomas, and E. Hafen, 2000   Genetic and biochemical characterization of dTOR, the Drosophila homolog of the target of rapamycin. Genes Dev. 14: 2689–2694.

Ono, H., K. F. Rewitz, T. Shinoda, K. Itoyama, A. Petryk et al., 2006   Spook and Spookier code for stage-specific components of the ecdysone biosynthetic pathway in Diptera. Dev. Biol. 298: 555–570.

Parker, N. F., and A. W. Shingleton, 2011 The coordination of growth among Drosophila organs in response to localized growth-perturbation. Dev. Biol. 357: 318–325.

Parkin, C. A., and B. Burnet, 1986 Growth arrest of Drosophila melanogaster on erg-2 and erg-6 sterol mutant strains of Saccharomyces cerevisiae. J. Insect Physiol. 32: 463–471.

Poodry, C. A., and D. F. Woods, 1990 Control of the developmental timer for Drosophila pupariation. Rouxs Arch. Dev. Biol. 199: 219–227.

Porcheron, P., M. Moriniere, J. Grassi, and P. Pradelles, 1989 Development of an enzyme immunoassay for ecdysteroids using acetylcholinesterase as label. Insect Biochem. 19: 117–122.

Rahn, P., 1972 Untersuchungen zur Entwicklung von Ganz und Teilimplantaten der Flugelimaginalscheibe von Ephestia kuhniella Z. Wilhelm Roux'. Arch. 170: 48–82.

Schubiger, G., 1971 Regeneration, duplication and transdetermination in fragments of the leg disc of Drosophila melanogaster. Dev. Biol. 26: 277–295.

Simmons, L. W., and D. J. Emlen, 2006 Evolutionary trade-off between weapons and testes. Proc. Natl. Acad. Sci. USA 103: 16346–16351.

Simpson, P., P. Berreur, and J. Berreur-Bonnenfant, 1980 The initiation of pupariation in Drosophila: dependence on growth of the imaginal discs. J. Embryol. Exp. Morphol. 57: 155–165.

Smith-Bolton, R. K., M. I. Worley, H. Kanda, and I. K. Hariharan, 2009 Regenerative growth in Drosophila imaginal discs is regulated by Wingless and Myc. Dev. Cell 16: 797–809.

Stern, D. L., and D. J. Emlen, 1999 The developmental basis for allometry in insects. Development 126: 1091–1101.

Stieper, B. C., M. Kupershtok, M. V. Driscoll, and A. W. Shingleton, 2008 Imaginal discs regulate developmental timing in Drosophila melanogaster. Dev. Biol. 321: 18–26.

Warren, J. T., Y. Yerushalmi, M. J. Shimell, M. B. O'Connor, L. L. Restifo et al., 2006 Discrete pulses of molting hormone, 20-hydroxyecdysone, during late larval development of Drosophila melanogaster: correlations with changes in gene activity. Dev. Dyn. 235: 315–326.

Yakubovich, N., and E. A. Silva, and P. H. O'Farrell, 2010 Nitric oxide synthase is not essential for Drosophila development. Curr. Biol. 20: R141–R142.

Communicating editor: I. K. Hariharan

GENETICS

Nitric Oxide Synthase Regulates Growth Coordination During *Drosophila melanogaster* Imaginal Disc Regeneration

Jacob S. Jaszczak, Jacob B. Wolpe, Anh Q. Dao, and Adrian Halme

<div align="center">**File S1**</div>

<div align="center">**Additional Methods**</div>

Measurement of growth parameters

Time to pupariation, the time at which half the population had pupated, was calculated by recording the number of pupariated individuals every 12hrs. For measuring imaginal tissue area, tissues were dissected in phosphate-buffered saline (PBS), fixed in 4% paraformaldehyde, mounted in glycerol, imaged by DIC on a Zeiss Axioplan2 microscope, and measured in ImageJ (NIH). The area of staged larvae was imaged, after a 10min treatment in PBS at 80°, on an Olympus DP21 microscope digital camera when viewed from the dorsal aspect, and measured in ImageJ.

Indirect immunofluorescence

Dissected tissues were fixed for 20 minutes in 4% paraformaldehyde, washed in PBS with 0.3% Triton-X100 to permeablize cells, treated with primary antibodies (overnight at 4°; rabbit anti-cleaved Caspase-3 (Asp175) 1:100, Cell Signaling Technology, MA), and secondary antibodies (4 hrs at room temperature). Cell death detection by TUNEL with TMR red fluorescent probe (Hoffmann-La Roche, Basel, Switzerland) was preformed following manufacturer instructions. Labeling buffers were mixed with secondary antibody stain and incubated for 2hrs at 37°.

Ecdysone measurements

Ecdysone levels in third instar larvae were quantified using a competitive enzyme immunoassay (Cayman Chemicals, MI) as described previously (Hackney *et al.* 2012).

NADPH-diaphorase assay

NOS enzymatic activity was detected by measuring NADPH-diaphorase activity through an adapted method (Elphick 1997). Tissues were fixed for 1hr in 4% paraformaldehyde and then permeablized in 0.3% Triton X-100 for 20min. Fixed tissues were suspended in NADPH-diaphorase staining solution in the dark for 15min, then washed in PBS, mounted in 80% glycerol, and imaged by DIC.

PCR

Semi-quantitative PCR

RNA was isolated from staged larvae using TRIzol reagent treatment (Invitrogen-Life Technologies, CA) followed by RNeasy cleanup (Qiagen, Limburg, Netherlands) and DNase treatment with the Turbo DNase-kit (Ambion-Life Technologies, CA). RNA yield was quantified by using UV spectroscopy to measure A260. cDNA template for RT-PCR was generated using 1μg sample RNA as a substrate for Roche Transcriptor first strand cDNA synthesis using poly dT primers. Polymerase chain reaction (PCR) was performed with TaKaRa Ex Taq DNA Polymerase (Takara, Otsu, Japan)

in a MJ research PTC-200 DNA Engine Cycler. Conditions for amplification were as follows: 94° for 2 minutes, then 94° for 15 seconds, 60° for 15 seconds, and 72° for 15 seconds for 23 cycles with Tubulin primers or 31 cycles with E75B primers. Amplified products were then identified by electrophoresis on a 3% agarose gel and visualized with SYBR Green (Life Technologies, CA) through epifluorescent analyzer (Fujifilm Intelligent Lightbox LAS-3000). Relative expression differences were measured in ImageJ in relation to tubulin expression. Primers: E75B (Moeller *et al.* 2015), tubulin (tub-L CTCATAGCCGGCAGTTCG)(tub-R GATAGAGATACATTCACGCATATTGAG).

Quantitative RT-PCR

RNA was isolated and cDNA was generated as described above except for Fig. S7, which used ReliaPrep™ RNA Cell and Tissue Miniprep Systems (Promega) and poly dT primers with random hexamer primers. cDNA was analyzed using a Mastercycle EP Replex real-time PCR system (Eppendorf). Fold change was calculated relative to tubulin expression by the -ΔΔCt method [53]. Isolates were taken from at least three sets of larval stagings to calculate the mean fold change. Two to three independent RNA isolations were assayed within each staging and used to calculate standard error of the mean across stagings. Primers: E74B (Colombani *et al.* 2015) , spookier (spo-L CGGTGATCGAAACAACTCACTGG, spo-R GGATGATTCCCGAGGAGAGCAG), disembodied (dib-L AGGCTGCTGCGTGAATACG, dib-R TCGATCAGCACTGGAGCATC).

Ecdysone media

Exogenous application of ecdysteroid was preformed as previously described (Halme *et al.* 2010). Briefly, larvae were transferred at 80hrs AED (*Bx>eiger, Tub>dilp8, Bx>dilp8, hs>NOS^{mac}*) or 124hrs AED (*phm>NOS*) to either 0.6 mg 20-hydroxyecdysone (Sigma) dissolved in 90% ethanol/ml of media, or an equivalent volume of ethanol alone. For ecdysone restriction assays, a defined yeast media was prepared with the erg-6 mutant yeast strain, sucrose, and agar (Bos *et al.* 1976, Parkin *et al.* 1986), and larvae were transferred from standard media to erg6$^{-/-}$ or erg6$^{+/-}$ media at 80hrs AED.

Supporting Information Literature Cited

Elphick MR, 1997 Localization of nitric oxide synthase using NADPH diaphorase histochemistry. Methods Mol Biol. 172:153–8.

Moeller ME, Danielsen ET, Herder R, O'Connor MB, Rewitz KF, 2013 Dynamic feedback circuits function as a switch for shaping a maturation-inducing steroid pulse in Drosophila. Development. 140:4730–9.
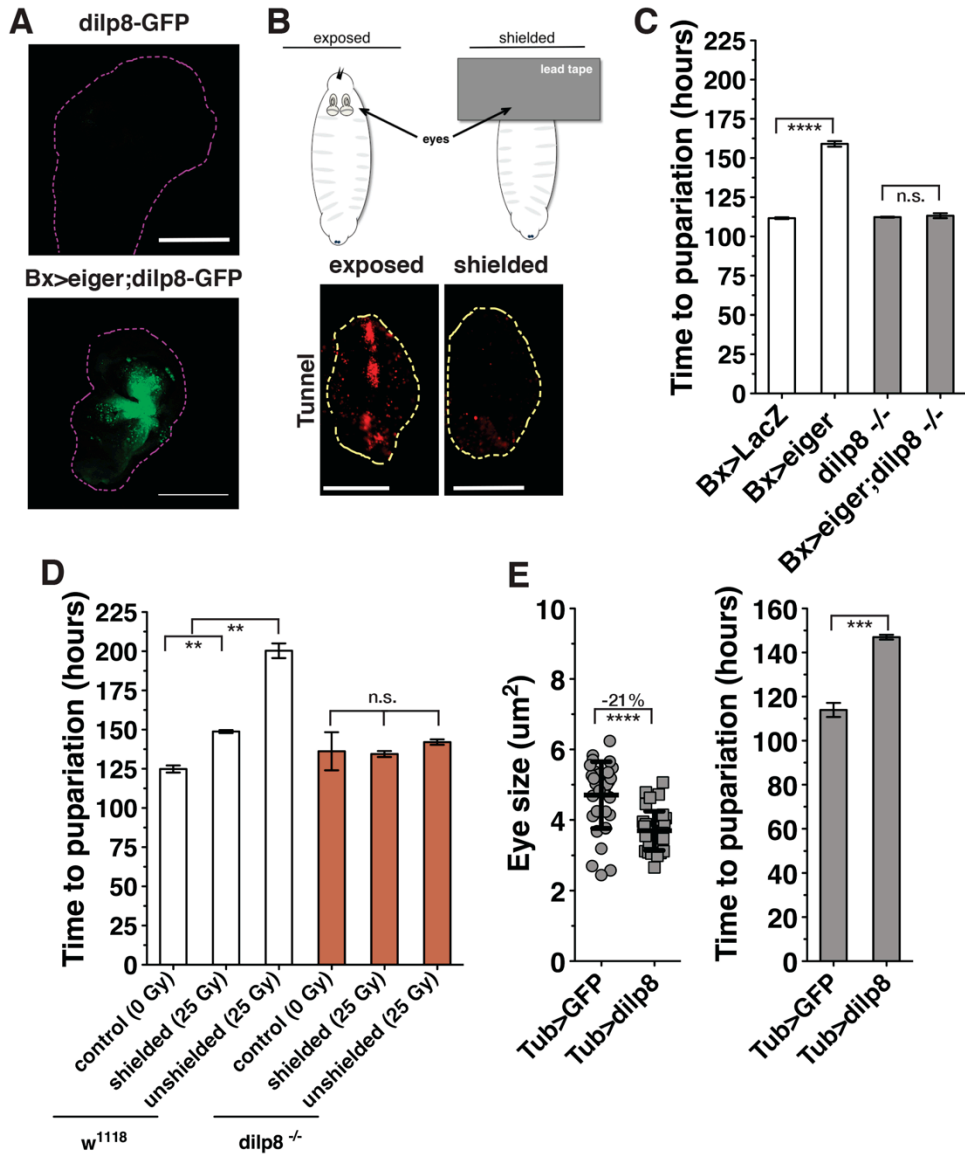
Figure S1. Imaginal disc growth inhibition during either Eiger-induced damage or targeted irradiation is dependent on Dilp8. (A) Dilp8 expression is increased in Eiger-misexpressing wing imaginal discs. Dilp8 expression is visualized in control (*dilp8-GFP*) and Eiger-misexpressing (*Bx>eiger;dilp8-GFP*) wing discs (outlined) using the *dilp8-GFP* enhancer trap (BL33079). Scale bars = 100μm. (B) Illustration of the targeted irradiation method that produces damage in the posterior tissues while protecting anterior tissues from ionizing radiation. Lead shielding protects eye imaginal discs from X-irradiation induced apoptosis. Levels of apoptosis measured by TUNEL staining (red) in eye imaginal discs (outline) isolated from larvae either completely exposed to X-rays, or partially shielded with lead tape to protect anterior tissues from direct damage. Scale bars = 100μm. (C and D) Developmental delay resulting from targeted wing damage (*Bx>eiger*) or targeted irradiation is dependent on *dilp8*. Measurement of pupariation timing for larvae with targeted wing expression of *eiger* (*Bx>eiger*) or targeted irradiation (shielded) damage, in larvae homozygous for *dilp8-GFP* [-/-,] or in WT control larvae is shown. (E) Eye imaginal disc size measured at 104hr AED following systemic misexpression of *dilp8* (*Tub>dilp8*) or in control larvae (*Tub>GFP*) is shown. Measurement of pupariation timing for larvae with systemic (*Tub>dilp8*) misexpression of *dilp8* is shown. Statistical analysis: Time in C, D and E, triplicates +/- SEM. E, growth mean +/- SD. * p<0.05, ** p<0.01, ****p<0.001 calculated by two-tailed Student's t-test, except for shielding experiments in D, calculated by one-way ANOVA with Tukey's post-test.
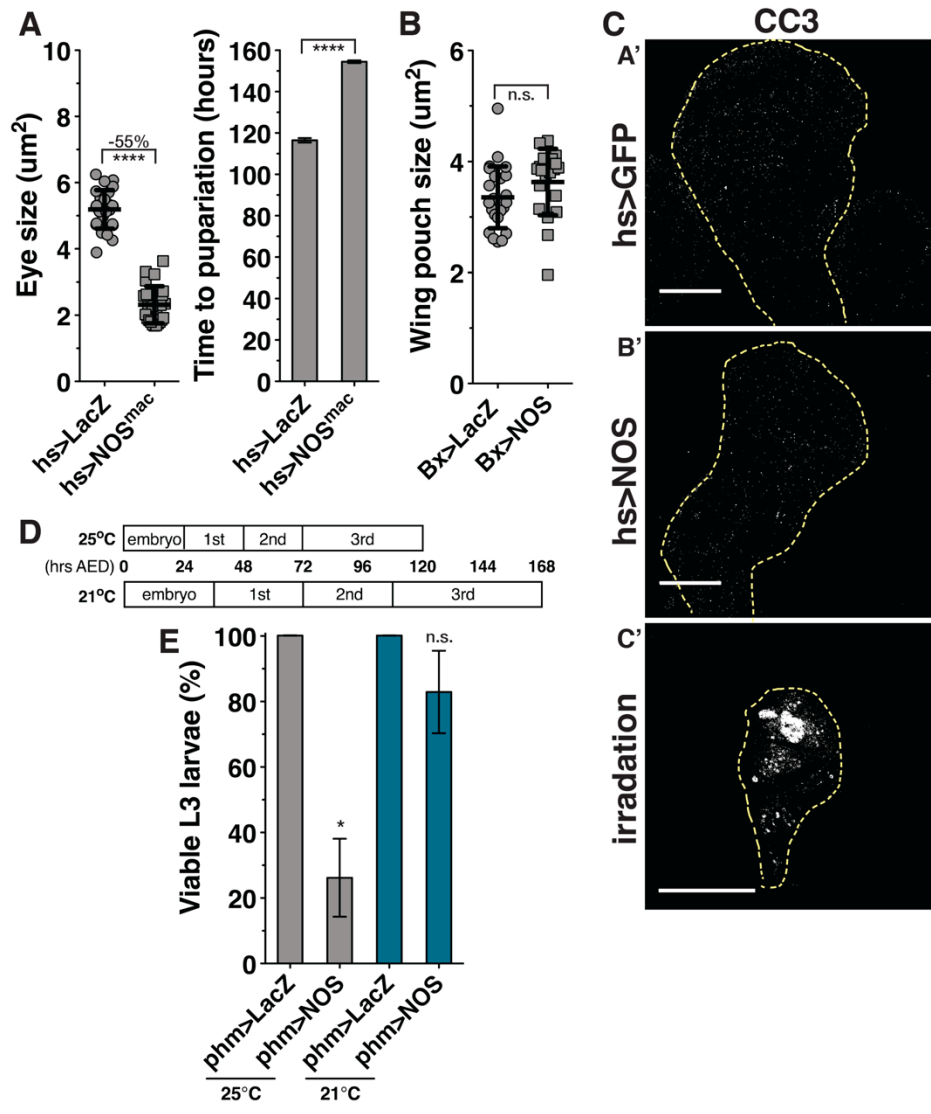
Figure S2. NOS non-autonomously regulates imaginal disc growth. (A) Systemic misexpression of mouse macrophage *NOS* (*NOS^mac*) reduces imaginal disc growth and delays developmental timing. Control (*hs>LacZ*) and *hs> NOS^mac* expressing larvae were raised at 25° and eye imaginal disc sizes was measured at 104hr AED. (B) *NOS* overexpression in the wing disc does not reduce growth. Targeted misexpression of *NOS* to the pouch of the wing imaginal tissue (*Bx>NOS*) is not sufficient to reduce growth of the wing pouch, nor wing area (data not shown). Wing imaginal discs measured at 104hr AED from larvae with targeted expression of *NOS* in the wing (*Bx>NOS*) and control (*Bx>LacZ*) larvae. (C) Systemic *NOS* misexpression does not induce cell death. Systemic *NOS* misexpression (*hs>NOS*) does not induce cell death in the wing discs. Cleaved caspase staining (CC3) in wing discs (outlines) isolated at 104hr AED. Control (*hs>GFP*) and *NOS* misexpression larvae (*hs>NOS*) that had been heat shock treated at 76hr AED, or larvae irradiated with 25 Gy as positive control for cell death (irradiation). Scale bars = 100μm. (D) Rearing larvae at 21° slows developmental time by approximately a factor of 1.5x that of developmental time at 25°. Instar transitions estimated from time to pupation and observations of larval size. (E) *NOS* overexpression in the PG at 21° increases larval survival into the 3rd instar (L3). *phm>NOS* larvae raised at 25° die before the third instar. Rearing *phm>NOS* larvae at 21° increased the number of larvae that progress to the third instar. Percent viable L3 *phm>NOS* and control (*phm>LacZ*) larvae raised at 25° and 21°. Statistical analysis: A and C, mean +/- SD. Time, mean of triplicate experiments +/- SEM. D, mean +/- SEM of three replicates. * p<0.05, ****p<0.001 calculated by two-tailed Student's t-test.

J.S. Jaszczak *et al.*
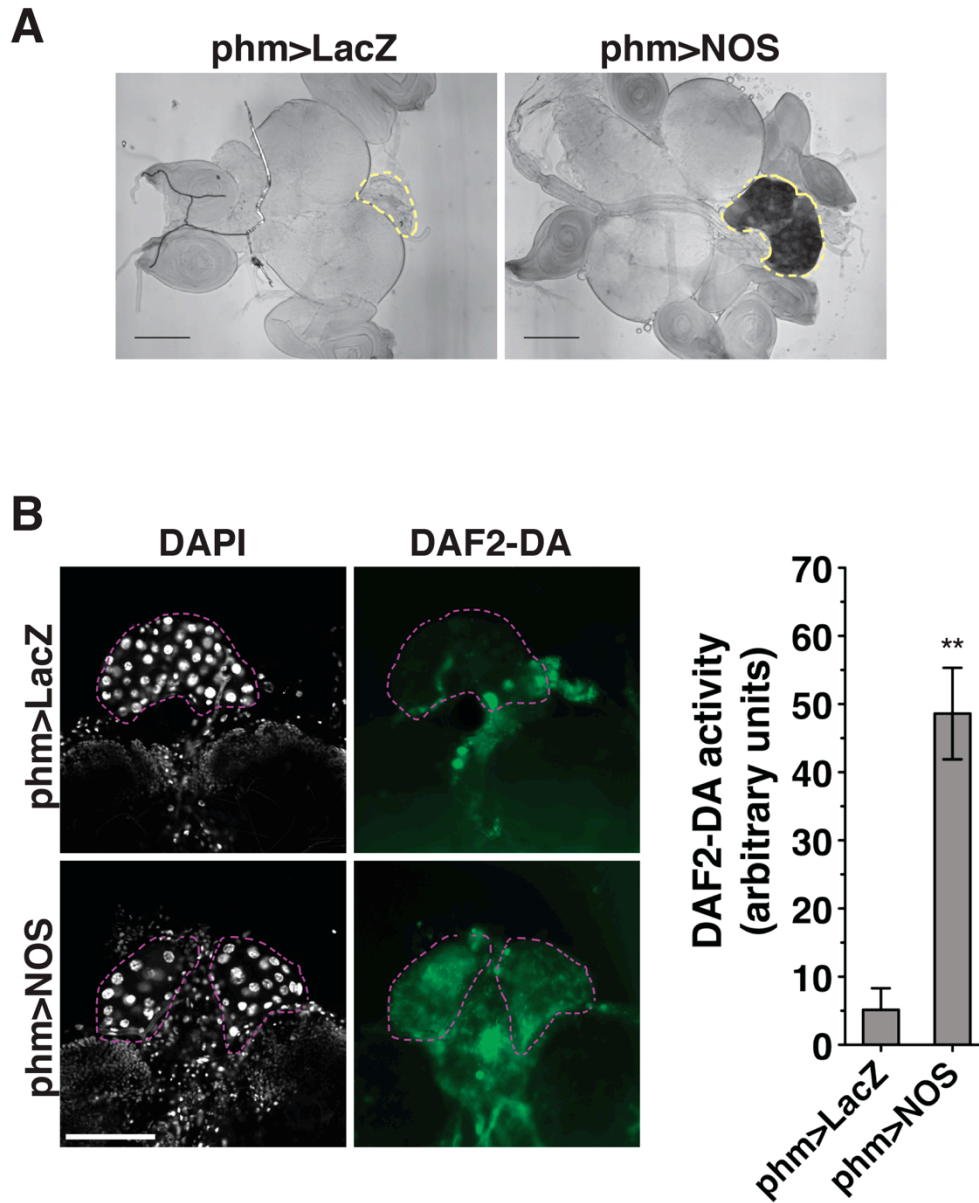
Figure S3. DAF2-DA assay for detection of NO production. (A) NOS enzymatic activity visualized by NADPH-diaphorase staining in targeted overexpression of NOS to the PG cells (outlined) (*phm>NOS*) and control (*phm>LacZ*). Larvae were raised at 21° and brain complexes were dissected from wandering larvae. Scale bars = 200μm. (B) *NOS* overexpression in the PG (*phm>NOS*) increases NO production in the PG cells (outlined). Measurement of nitric oxide (NO) production by the fluorescent reporter DAF2-DA. Larvae were raised at 21° and brain complexes with the PG were isolated and stained at 117hr AED. Scale bar = 100μm. n: *phm>LacZ* = 29, *phm>NOS* = 30. Statistical analysis: mean +/- SEM. ** p<0.01 calculated by two-tailed Student's t-test.
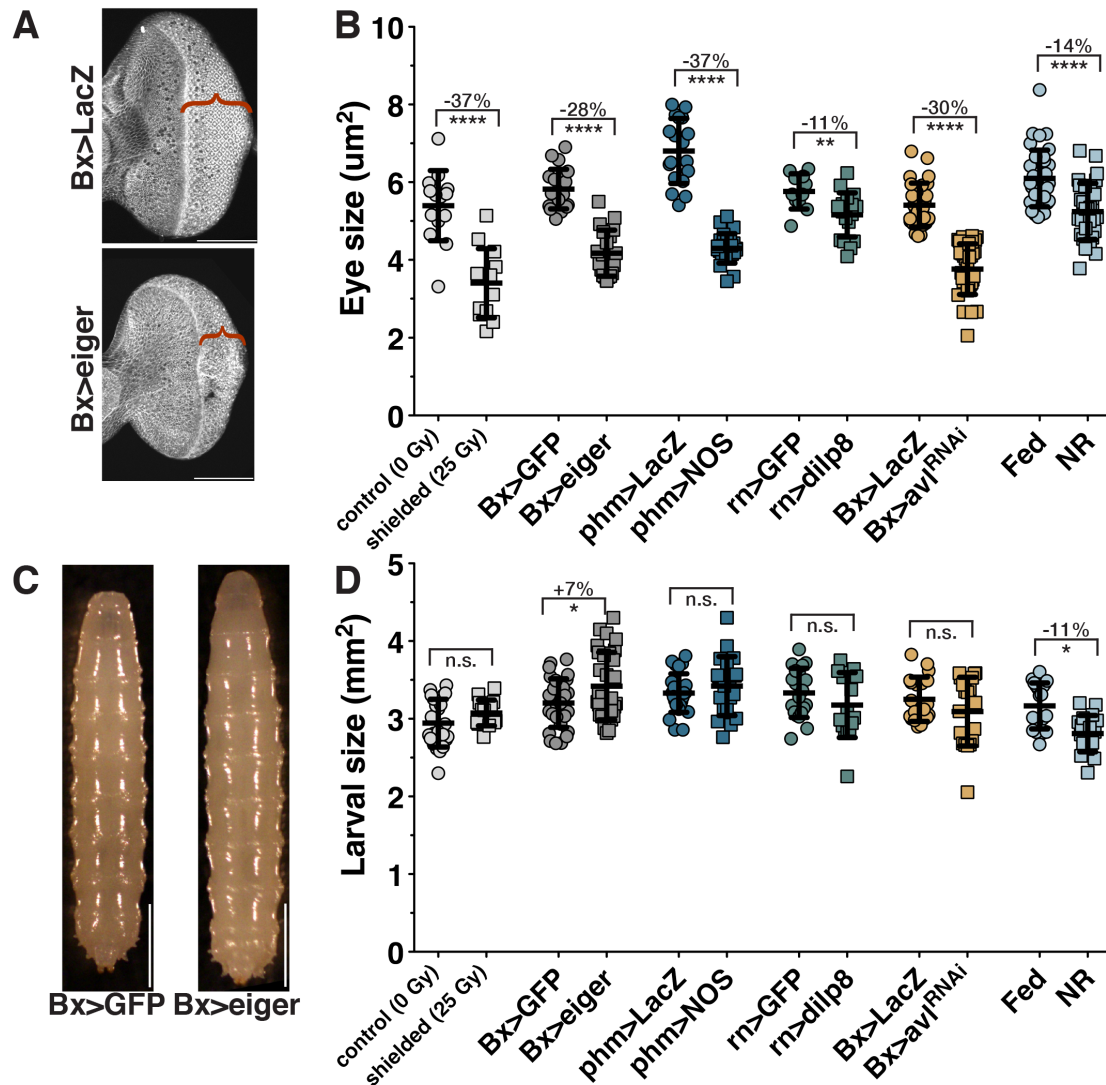
Figure S4. The regeneration checkpoint selectively restricts imaginal tissue growth. (A) Growth reduction and developmental delay of undamaged eye imaginal discs in larvae with targeted tissue damage in the wings (*Bx>eiger*) and control larvae (*Bx>GFP*). Eyes were isolated at 104hr AED and stained with rhodamine-labeled phalloidin. Brackets highlight the progression of the morphogenetic furrow in each disc. Scale bar = 100 μm. (B) Measurement of eye imaginal disc size following nutrient restriction (NR) or multiple distinct activators of the regeneration checkpoint including: targeted irradiation with 25 Gy (shielded), expression of pro-inflammatory signal (*Bx>eiger*), expression of NOS in the PG (*phm>NOS*), wing-targeted expression of dilp8 (*rn>dilp8*), and wing-targeted neoplastic transformation (*Bx>avl^RNAi*). Larvae were raised at 25° and eye imaginal discs were isolated at 104hr AED for measurement of all experiments except for the following: *rn>GFP* and *rn>dilp8*, raised at 29° and eye discs were dissected and measured at 80hr AED to maximize dilp8 overexpression and the systemic growth phenotype. *phm>LacZ* and *phm>NOS* larvae were raised at 21° and eye discs were dissected and measured at 142hr AED to reduce *NOS* overexpression and permit analysis of third instar growth phenotypes. (C) The regeneration checkpoint does not restrict larval growth. *Bx>eiger* and control larvae isolated at 104hr AED. Scale bar = 1 mm. (D) Measurement of larval growth. Larvae were raised and isolated for measurement as the same conditions in B. Statistical analysis: B and D, mean +/- SD. * p<0.05, ** p<0.01, ****p<0.001 calculated by two-tailed Student's t-test.
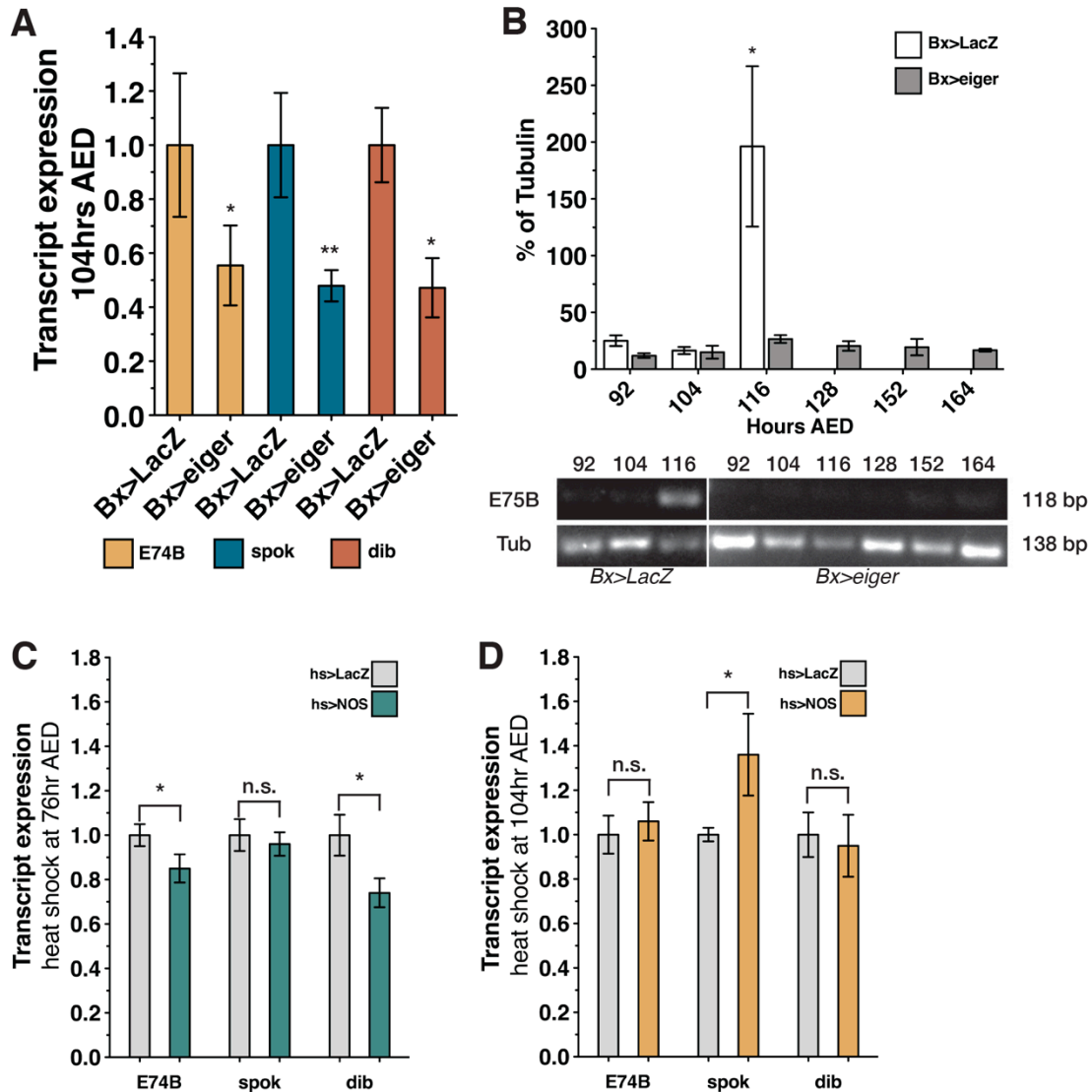
Figure S5. NOS inhibits ecdysone synthesis during the feeding period, and promotes ecdysone production post-feeding. (A) Regeneration checkpoint activation reduces ecdysone signaling and Halloween gene transcription. Transcription of ecdysone-induced *E74B*, a reporter for early ecdysone levels during the third larval instar, in control larvae (*Bx>LacZ*) and larvae with targeted tissue damage (*Bx>eiger*). Transcription of *spok* and *dib*, ecdsyone biosynthesis genes, in control larvae (*Bx>LacZ*) and larvae with targeted tissue damage (*Bx>eiger*). (B) Targeted tissue damage (*Bx>eiger*) suppresses transcription of the nuclear hormone receptor (*E75B*) involved in the initiation of pupariation. Transcript levels of *E75B* and *tubulin* measured by semi-quantitative PCR in *Bx>LacZ* and *Bx>eiger* larvae from 92h AED until the end of the larval growth period are shown. (C) Expression of *NOS* early, during the larval feeding period, restricts ecdysone biosynthesis genes and signaling. *NOS* was systemically expressed by heat shock (*hs>NOS*) at 76hr AED and ecdysone signaling (*E74B*) and Halloween gene (*spok* and *dib*) transcription was measured by qRT-PCR at 116hr AED. (D) Expression of *NOS* late, during the wandering period promotes ecdysone biosynthesis gene transcription. *NOS* was systemically expressed by heat shock (*hs>NOS*) at 104hr AED and *E74B*, *spok*, and *dib* transcription was measured by qRT-PCR at 116hr AED. Statistical analysis: A, mean of triplicates +/- SEM. * $p<0.05$, ** $p<0.01$, calculated by paired one-tailed student's t-test. B, mean of two isolation replicates +/- SEM. * $p<0.05$, calculated by two-way ANOVA. C and D, mean of duplicates +/- SEM. * $p<0.05$, calculated by paired one-tailed student's t-test.
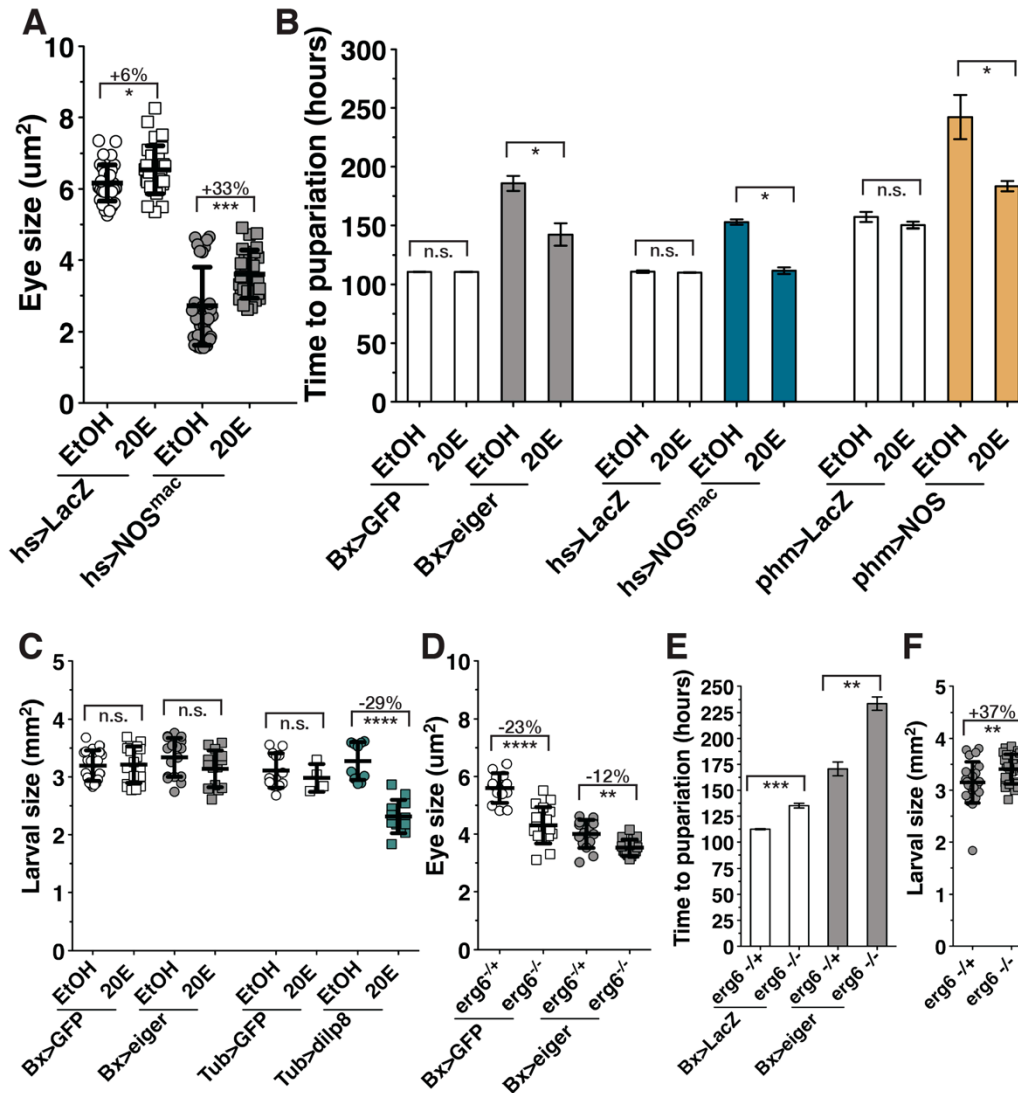
Figure S6. Ecdysone regulates larval growth and developmental time. (A) Ecdysone levels are rate-limiting for imaginal disc growth during the systemic NOS^{mac} misexpression. 20E rescues growth restriction induced by $hs>NOS^{mac}$ compared to control ethanol only fed larvae (EtOH). Larvae were heat shocked at 76hr and eye discs were measured at 104hs AED. (B) Ecdysone rescues developmental delay induced by $Bx>eiger$, $hs>NOS$, and $phm>NOS$. Measurement of time to pupariation for larvae raised in food with supplemental ecdysone (20E) or control food (EtOH). (C) Supplemented 20E only significantly reduces larval tissue growth in $Tub>dilp8$ larvae. Measurement of larval growth at 104hr AED in larvae raised in food with supplemental ecdysone (20E) or control food (EtOH) is shown. (D) Non-additive effects of wing damage and ecdysone reduction on eye imaginal disc growth suggest convergent mechanisms. Measurement of eye imaginal disc size in larvae with targeted wing damage ($Bx>eiger$) and control larvae ($Bx>GFP$). Larvae were transferred at 80hr to food lacking steroid ecdysone precursor ($erg6^{-/-}$) or control food ($erg6^{-/+}$). (E) Restriction of ecdysone synthesis ($erg6^{-/-}$) extends the time to pupation when compared to permissive synthesis conditions ($erg6^{-/+}$) for both control ($Bx>GFP$) and $Bx>eiger$. (F) $erg6^{-/-}$ inhibition of ecdysone increases the growth rate of larval tissues. Measurements of imaginal disc growth and larval growth were at 104hr AED. Statistical analysis: A, C, D, and F mean +/- SD. B and E, triplicates +/- SEM. * $p<0.05$, ** $p<0.01$, ***$p<0.0005$, ****$p<0.001$ calculated by two-tailed Student's t-test.